



¹⁰Be age control of glaciation in the Beartooth Mountains, USA from the latest Pleistocene through the Holocene

Aaron M. Barth¹, Elizabeth G. Ceperley², Claire Vavrus², Shaun A. Marcott², Jeremy D. Shakun³,
Marc W. Caffee^{4,5}

5 ¹Department of Geology, Rowan University, Glassboro, NJ, USA

²Department of Geoscience, University of Wisconsin – Madison, Madison, WI, USA

³Department of Earth and Environmental Sciences, Boston College, Chestnut Hill, MA, USA

⁴Department of Physics and Astronomy, Purdue University, West Lafayette, IN, USA

⁵Department of Earth, Atmospheric, and Planetary Sciences, Purdue University, West Lafayette, IN, USA

10 *Correspondence to:* Aaron M. Barth (bartha@rowan.edu)

Abstract. Alpine glaciers in the western United States are often associated with late-Holocene Little Ice Age (LIA) advances. Yet, recent studies have shown many of these glacial landforms are remnants of latest-Pleistocene retreat with only the most cirque-proximal moraines preserving LIA activity. Additionally, the timing and magnitude of glacial advances during the Neoglacial-LIA interval remains uncertain with presumed maximum extents occurring during the LIA driven by lower Northern Hemisphere insolation levels. Here we present ¹⁰Be surface exposure ages from a glacial valley in the Beartooth Mountains of Montana and Wyoming, United States. These new data constrain the presence of the glacier within 2-3 km of the cirque headwalls by the end of the Pleistocene with implications for large-scale retreat after the Last Glacial Maximum. Cirque moraines from two glaciers within the valley preserve a late-Holocene readvance with one reaching its maximum prior to 2.1 ± 0.2 ka and the other 0.2 ± 0.1 ka. Age variability among the moraines demonstrates that not all glaciers were largest during the LIA and presents the possibility of regional climate dynamics controlling glacial mass balance.

1 Introduction

25 Glacial retreat is one of the clearest indicators of the climate system's response to recent global warming. Photographic and satellite imagery of reductions in global glacial extent from the past century demonstrate this widespread phenomenon (Bolch, 2007; Catania et al., 2018). Within the last two decades alone, the rate of ice loss from mountain glaciers has doubled (Hugonnet et al., 2021). However, analysis of glacier sensitivity to climate change is limited by the instrumental record, which only goes back decades (Braumann et al., 2020). We are therefore reliant on geologic records of past glacial activity to determine the influence of anthropogenic warming on glacier mass balance relative to natural variability. In the early Holocene, glaciers within the western United States (U.S.) and Canada were at minimum lengths, similar to modern, with peak Northern Hemisphere (NH) summer insolation values contributing to the retreat (Solomina et al., 2015). Reactivation of glaciation after 6 ka ("Neoglacial") occurred as glaciers advanced to their greatest Holocene extent (Porter and Denton, 1967; Solomina et al., 2016, 2015). Relative to the last glacial period, the Holocene is considerably more stable in terms of its climate variability. However, variable

35



timing of glacier maximum extent throughout the Neoglacial suggests other mechanisms besides NH insolation. Well-dated records of late-Holocene glaciation are therefore required to accurately assess forcing mechanisms for the Neoglacial.

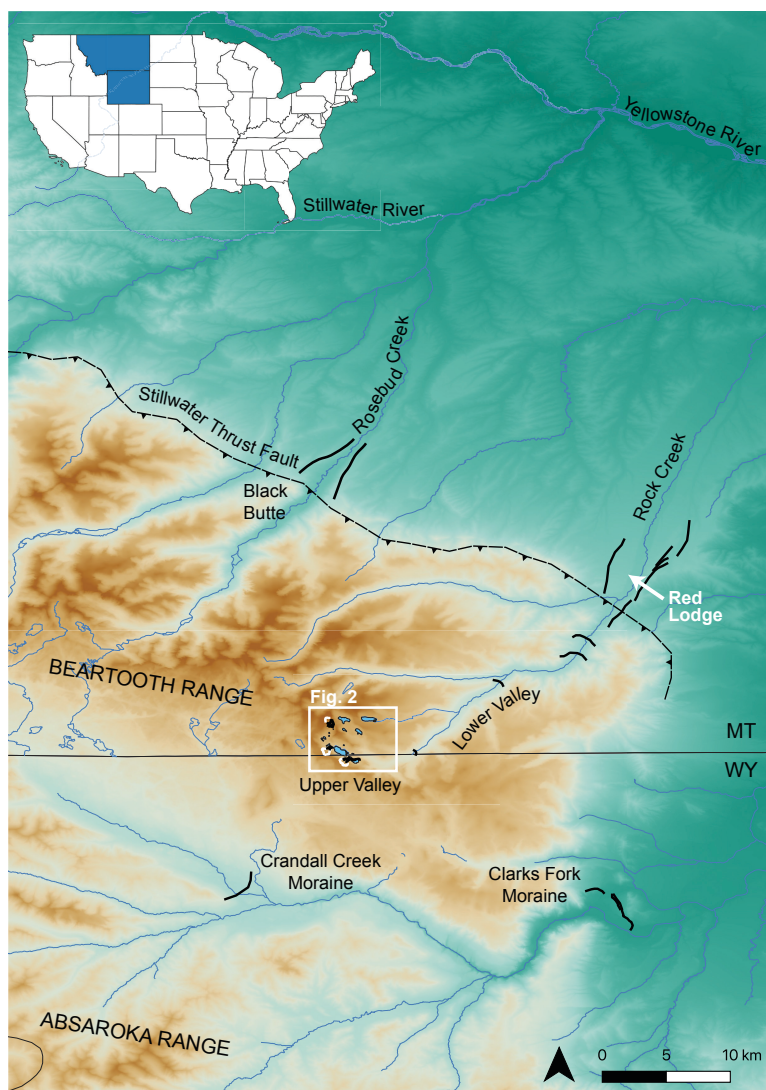
40 Many mountain ranges of the western U.S. remained below the southern reaches of the Laurentide Ice Sheet during the Last Glacial Maximum (LGM, 26 – 19 ka; Clark et al., 2009) where numerous alpine glaciers and icecaps nucleated (Laabs et al., 2020). LGM glacial positions are recorded as down valley moraines extending as much as 50 km from the cirques while younger, high-elevation glacial landforms are preserved within 1-2 km of the headwall (Davis, 1988; Davis et al., 2009). These younger glacial deposits were originally thought to record Neoglaciation, but
45 and earliest Holocene glaciation (Marcott et al., 2019). The questions then arise: what is the record of late Holocene glaciation in the western U.S., if any exists at all? What does it tell us about the response of mountain glaciers to climatic forcings throughout the Holocene, and were they sufficient to permit glacial regrowth?

50 Here we present ^{10}Be exposure ages from high-elevation glacial landforms in the Beartooth Mountains of Montana (MT) and Wyoming (WY) to determine the timing of glaciation in this sector of the western U.S. Together with previously published ages on downvalley LGM moraines, this new chronology sheds light on the rate and magnitude of glacier retreat during the last deglaciation as well as potential Neoglacial regrowth during the late Holocene.

2 Geologic and geomorphic background

55 The Beartooth Mountain range extends from southwestern MT into northern WY and is a broadly arcuate mountain range reaching ~30 km at its widest. At its base, the Mill Creek-Stillwater Fault Zone separates the northern foothills of the Beartooths from the Great Plains (Fig. 1; Bevan, 1923; Montgomery and Lytwyn, 1984) with ~1800 m relief between the Plains (~1800 m asl) and the highest elevations in the mountain range (>3600 m asl). High plateaus have been dissected by fluvial and glacial erosion. Numerous cirques and northward-oriented glacial valleys
60 are present within the Beartooths, whereas the Absoroka Range to the south exhibits more south- and eastward-oriented glacial valleys. The eastern portion of the mountain range is predominantly Archean quartz-rich granitic gneisses and migmatites with inclusions of metasedimentary and metaigneous rocks (Van Gosen et al., 2000). Course pegmatitic dikes are common throughout the region (Bevan, 1923).

65 Glacial landforms in the mountain range record multiple phases of glaciation, including the Bull Lake (Marine Isotope Stage (MIS) 6), and Pinedale (MIS 2) glaciations. Bull Lake glaciation within the northeast sector of the Beartooths is recorded as remnant outwash terraces of higher elevation to those of the younger Pinedale terraces (Ballard, 1976). Morainal evidence, however, is sparse for Bull Lake glacier limits and is suggestive of similar, or lesser, glacial extents to Pinedale advances (Licciardi and Pierce, 2018). During the last glaciation, high-elevation ice flowed southward to the Yellowstone Plateau where it coalesced with similar glaciers from the surrounding mountains
70 forming the Yellowstone ice cap, which acted as an ice divide at the LGM (Licciardi and Pierce, 2018, 2008). Numerous, long (>20 km) glacial valleys are present along the periphery of the Greater Yellowstone Glacial System (GYGS), including those of the northern Beartooths. Glacial deposits including erratics, moraines, and outwash



75 **Figure 1 - Regional Map - Map of the Beartooth Mountain range in Montana and Wyoming, United States. Brown colors indicate higher elevation, and green colors lower elevation. Solid black lines show the location of prominent moraines including those mapped by Graf (1971) in the Rock Creek drainage. Inset map shows the location of Montana (MT) and Wyoming (WY) highlighted in blue. Elevation data from the U.S. Geological Survey 3D Elevation Program (U.S. Geological Survey, 20171130, USGS 13 arc-second n46w110 1 x 1 degree: U.S. Geological Survey).**

80

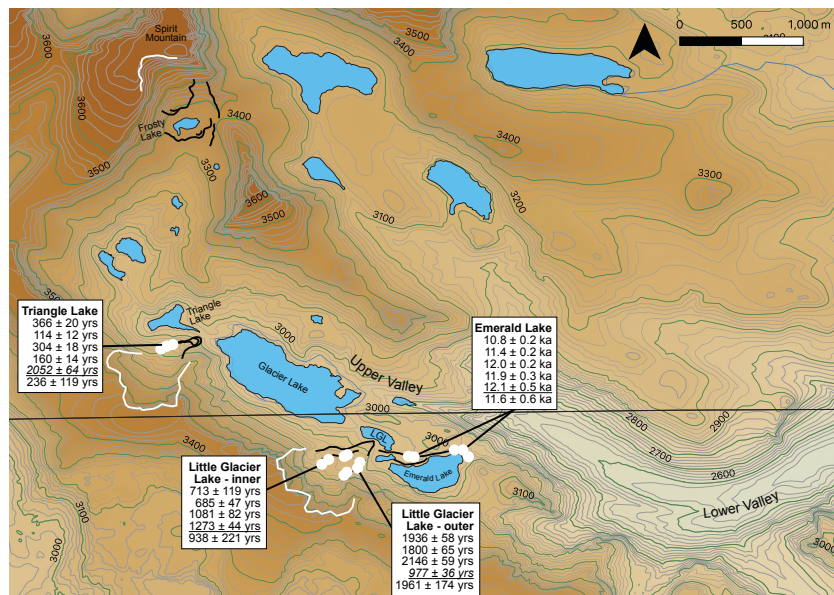
terraces are common within these valleys and provide abundant geologic evidence of past glacial activity from the LGM and deglaciation. Higher in the valleys, proximal to cirque headwalls, additional glacial evidence is preserved as sharp-crested moraines, rock glaciers, and protalus lobes (Davis, 1988; Graf, 1971). Most features are mapped within 1-2 km from cirque headwalls and may represent multiple phases of glaciation (Davis, 1988). Based on

85 geomorphologic characteristics, Graf (1971) identified such features in the Beartooths as two periods of late-Holocene



glaciation. However, geochronologic data are limited by relative-age methods and their associated uncertainties (Davis, 1988).

The Rock Creek drainage, a ~25 km long glacial valley, exits from the northeast corner of the Beartooth Range with associated cirque valleys, including Glacier Lake Valley (study area), located along the border between MT and WY and just north of Yellowstone National Park (Fig. 1 & 2). The lower portion of this drainage (herein referred to as the Lower Valley) is fed by five higher-elevation glacial cirques, trends southwest-northeast, and drains into the town of Red Lodge, MT. Sets of lateral moraines extend north from the valley mouth and bound the town on the eastern and western sides. The lateral moraines define an elongate and relatively narrow former glacier, and they are similar in morphology and size to moraines in valleys 25 km to the west beneath Black Butte. Outboard of the moraines, there are fluviially-modified hills unaffected by glacial activity, while outwash sediments between the lateral moraines suggest extensive meltwater drainage from the Lower Valley. A terminal moraine for this glacier is not preserved, likely due to erosion from meltwater flowing north to the Yellowstone River (Fig. 1). Graf (1971) mapped five moraines within the Lower Valley, although preservation is patchy, including stream breaches ranging from 70 m wide to as wide as the valley floor in some cases. Steep sloped, rocky walls define the valley width, which averages 1.5 to 2.0 km at its widest and narrows further upvalley. Occasional large (>1 m) boulders along the valley floor exhibit glacially-faceted surfaces and striations. The Lower Valley is gently sloped, gaining only 800 m of elevation from the Great Plains over 25 km.



105 **Figure 2 - Glacier Lake Valley map** - Map of the study area highlighting the names of important locations discussed in the paper. White lines indicate the cirque headwalls. Solid black lines show the location of moraines. Relative elevation shown using the same color scheme as Figure 1. White circles indicate the locations of surface exposure samples with their ages contained in the respective boxes. Mean age and standard deviation for each population located beneath the line in each box. Statistically identified outliers are italicized. LGL =



110 **Little Glacier Lake. Elevation data from the U.S. Geological Survey 3D Elevation Program (U.S. Geological Survey, 20171130, USGS 13 arc-second n46w110 1 x 1 degree: U.S. Geological Survey).**

There is a steep, 400 m-high transition from the Lower Valley to Glacier Lake valley (herein referred to as the Upper Valley), capped by an exposed, glacially-abraded, bedrock lip. Four lakes are located between 2960-2970 m asl within the Upper Valley (from east to west): Emerald Lake, Little Glacier Lake, Glacier Lake, and Triangle Lake (Fig. 2). Two of the lakes, Emerald Lake and Little Glacier Lake, are bounded by the bedrock lip to the north. To the south, Emerald Lake is bounded by an exposed bedrock cliff while Little Glacier Lake by a bouldery moraine. A deflated and curved boulder-covered moraine exists in the gentle topography between the two lakes (referred to as the Emerald Lake moraine) and is the stratigraphically oldest moraine in the Upper Valley (Graf, 1971). The location and size of Glacier Lake is controlled by steep rocky walls to the north and south with colluvial fans along the base of the southern wall. Two bedrock knobs separate Glacier Lake from Triangle Lake to the west, with morainal deposits restricting water flow between the two (Graf, 1971). To the northwest of Triangle Lake, a rounded and smoothed bedrock exposure increases elevation as the valley changes orientation to north-south and gains another ~450 m of elevation. A small cirque below the peak of Spirit Mountain (3744 m asl) contains a lake, Frosty Lake, and two moraines along both the down- and upvalley shores. The downvalley moraine is low-relief, bouldery, and rests on the cirque lip. The upvalley moraine is 50 m tall, sharp-crested, within 25 m of modern ice, and morphologically similar to the moraine at Triangle Lake. No prominent moraines are present between Triangle Lake and those at Frosty Lake.

The cirque near Little Glacier Lake preserves two moraines with an additional moraine in the cirque near Triangle Lake (Fig. 2). The moraines around Little Glacier Lake have high-angle lateral slopes of large (>1 m) angular boulders mixed with coarse to fine sands and all grain sizes in between (Fig. 3). The toe of the moraine is lower-relief (15 m), dominated by boulders, and rests along the southern shore of Little Glacier Lake. The left-lateral moraine rests on a bedrock outcrop at 3022 m asl (Fig. 3B). Ribbed crests of boulder deposits are found inboard of the left lateral moraine and maintain a similar elevation throughout. Between the lateral moraines, the surface elevation remains fairly consistent, with drastic changes in slope only along the distal sides of the moraines. While the moraine crests are easily defined, abundant boulder debris coverage within the moraine limits is suggestive of rock glacier activity or rockfall from over-steepened cliff faces. Small patches of modern ice are visible near the headwall but are covered in debris further down slope.

A steep-sloped moraine is found along the southern shore of Triangle Lake, ~1.2 km north of a cirque headwall containing a small (~0.1 km²), debris-covered glacier. The moraine increases in relief from 35 m near the terminus to 80 m along the lateral aspects and contains abundant coarse sands and gravels among numerous angular boulders (>0.4 m in height). The peak of the moraine is narrow and exhibits minimal deflation, yet occasional patches of grass and soil suggest the surficial deposits are not recent. From the terminus, the moraine curves to the east to intersect a near-vertical cliff face and is covered with boulders, some up to ~10 m in size. The western aspect of the moraine gains 130 m elevation before encountering a glacially-smoothed bedrock knob. Above the bedrock knob, the moraine continues another 60 m before reaching the glacier.

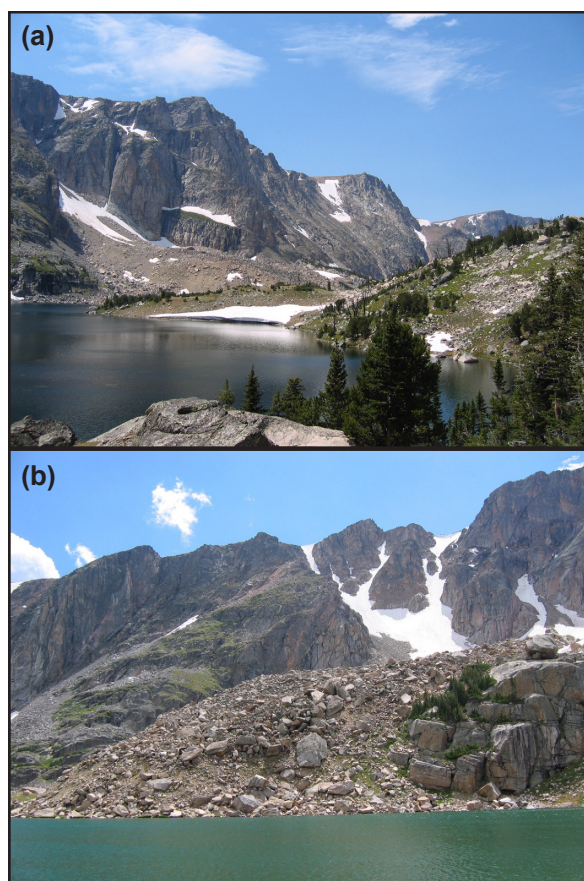


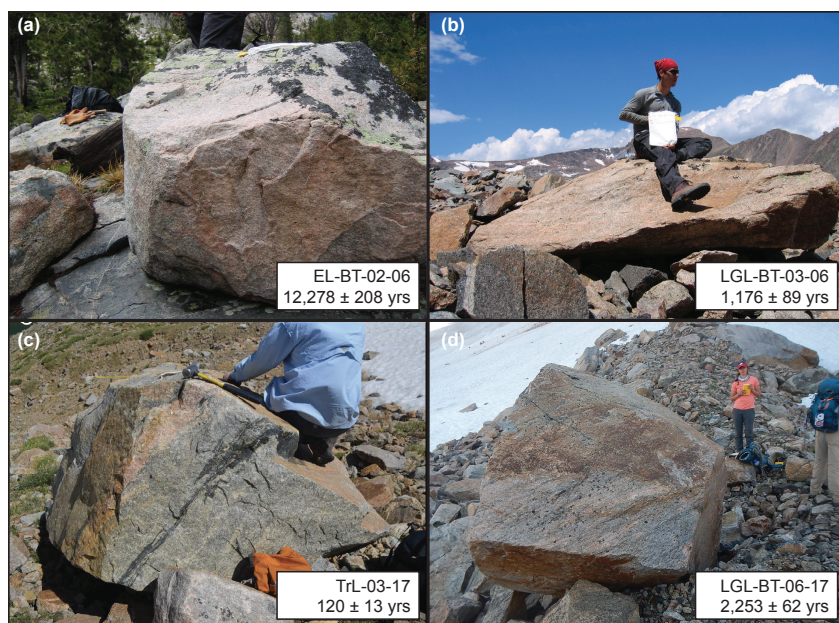
Figure 3 - Beartooth Moraines – (a) Emerald Lake moraine on the left with the Little Glacier Lake moraines in the distance. (b) Toe and left lateral aspect of the Little Glacier Lake moraine and bedrock knob.

150

3 Methods

To determine the timing of glaciation within Upper Valley, we sampled glacially-deposited boulders for cosmogenic ^{10}Be surface exposure dating from four moraines: one at Triangle Lake, two at Little Glacier Lake, and one at Emerald Lake moraine (Fig. 4). Samples were collected over two field seasons in 2006 (Emerald Lake and Little Glacier Lake) and 2017 (Triangle Lake and Little Glacier Lake) using hammer and tungsten carbide-tipped chisels. Strict sample selection criteria were followed to maximize the accuracy of nuclide accumulation representative of initial deposition by the glacier (Dunai, 2010; Gosse and Phillips, 2001). Boulders selected for sampling exhibited no signs of surficial erosion or pitting that would remove accumulated nuclides. Samples were limited to within the top five centimeters from flat-topped boulders to ensure highest rates of *in-situ* nuclide production. All samples were collected on or near the mapped moraine crest to minimize potential post-depositional movement and associated reduction of nuclide accumulation on the sampled surface. Each boulder was a minimum of 0.4 m in height with an average boulder height of 1.5 m. Potential boulder burial or exhumation is unlikely given boulder height and morphological characteristics of the moraines. Both the Little Glacier Lake and Triangle Lake moraines exhibit little

160



165 **Figure 4 - Sample boulders - Boulders sampled for ^{10}Be surface exposure dating discussed in this project. (a) EL = Emerald Lake. (b,d) LGL = Little Glacier Lake. (c) TrL = Triangle Lake. 1-sigma analytic uncertainty shown for each age.**

170 to no soil cover, which suggests exhumation of boulders from previous cover is unlikely. Latitude, longitude, and elevation were recorded for each sample using a handheld GPS unit and verified using high-resolution DEMs and topographic maps. Surface inclination of each sample was measured using a Brunton compass and topographic shielding was recorded in the field using a clinometer. Shielding scaling factors for each sample were calculated using the CRONUS online Topographic Shielding Calculator (http://stoneage.ice-d.org/math/skyline/skyline_in.html; Balco et al., 2008)

175 A total of 33 samples were collected over the two field seasons including two samples from the exposed bedrock at Triangle Lake, which exhibited glacial polishing. Eighteen samples were processed for ^{10}Be extraction that best represent our selection criteria: five boulders from Emerald Lake, four from the inner Little Glacier Lake moraine, four from the outer Little Glacier Lake moraine, and five from Triangle Lake.

180 Boulder samples were processed for ^{10}Be extraction at the University of Wisconsin – Madison. The sample processing procedures are adapted from laboratories at Oregon State University, the University of Vermont Cosmogenic Nuclide Laboratory, and the University of New Hampshire (Corbett et al., 2016; Kohl and Nishiizumi, 1992; Licciardi, 2000; Marcott, 2011). Each rock sample was sawed to isolate the top 2-5 cm, crushed and sieved to a 250-710 μm size fraction, magnetically separated, and etched in concentrated HCl and dilute HF/HNO₃ acid solutions. Chemical frothing was performed on all non-magnetic grains in order to isolate quartz from feldspar. The remaining quartz grains were isolated using additional HF/HNO₃ etches. Quartz purity was measured by inductively

185



coupled plasma optical emission spectroscopy (ICP-OES) at the University of Colorado-Boulder Department of Geological Sciences and the University of Wisconsin-Madison Water Science and Engineering Laboratory.

190 The chemically etched and pure quartz was dissolved in concentrated HF, after an addition of ^9Be carrier solution prepared from raw beryl (OSU White standard; ^9Be concentration of 251.6 ± 0.9 ppm) (Marcott, 2011). We used anion and cation exchange chromatography to separate Fe, Ti, and Al from Be, and BeOH was precipitated in a pH 8 solution. BeOH gels were converted to BeO by heating to 900-1000°C with a rapid incinerator, then mixed with Nb powder in quartz crucibles, and packed into stainless steel cathodes for accelerator mass spectrometry (AMS) analysis.

195 All $^{10}\text{Be}/^9\text{Be}$ ratios were measured at the Purdue University Rare Isotope Measurement Laboratory (PRIME Lab) and normalized to standard 07KNSTD3110, which has an assumed $^{10}\text{Be}/^9\text{Be}$ ratio of 2.85×10^{12} (Nishiizumi et al., 2007). Sample ratios were corrected using batch-specific blank values that ranged from 2.39×10^{-15} to 4.19×10^{-15} ($n = 3$; Table 1). ^{10}Be concentrations presented in Table 1 are corrected from process blanks.

200 Exposure ages are calculated using version 3.0 of the original online calculator as described in Balco et al. (2008; herein referred to as Version 3.0) and the time-dependent scaling scheme of Lifton et al. (2014; LDSn). We use the ^{10}Be production rate in quartz as determined from Promontory Point, UT (PPT; Lifton et al., 2015) based on proximity to the study site (~700 km) and high confidence in the quality of constraining samples. We note that a recent review of Western U.S. surface exposure ages follows similar methods for recalculating previous published data (Laabs et al., 2020; Licciardi and Pierce, 2018) including those for the GYGS. Wide-ranging rates of surface erosion experienced by glacial erratics are suggested in the literature with rates within the order of 0.0 to 0.1 cm ka^{-1} (Ballantyne and Stone, 2012). Based on the presumed young age of our sampled deposits, we assume surface erosion of the boulders was negligible and therefore do not account for it in our calculations. We follow the procedures outlined in Laabs et al. (2020) and assume the effects of snow cover to be negligible. Individual exposure ages are reported as years before collection date (per Version 3.0 calculations) and with 1-sigma analytical uncertainty. Moraine ages are reported as the arithmetic mean and standard deviation of the boulder ages to present a conservative uncertainty estimate. We note that distribution ages reported using error-weighted mean and uncertainty tend to favor younger exposure ages with lower analytical uncertainty which are more likely to be influenced by geological processes (e.g., surface erosion, post-depositional movement) leading to erroneously young ages (Barth et al., 2019; Laabs et al., 2020). Outliers are identified using Chauvenet's criterion and interquartile range tests.

215 4 Results

220 Resulting ^{10}Be exposure ages demonstrate glaciation within the Upper Valley from the latest Pleistocene and the late Holocene with all ages in stratigraphic order. Five exposure ages from the stratigraphically oldest moraine at Emerald Lake range from 11.3 ± 0.2 to 13.0 ± 0.5 ka (Table 1). Together these samples have a mean age and standard deviation of 12.5 ± 0.7 ka. We note that sample EL-BT-01-06 (11.3 ± 0.2 ka) is 0.9 ka younger than the next youngest sample (EL-BT-02-06; 11.4 ± 0.2 ka), yet cannot be rejected using either of the statistical tests. Removing sample EL-BT-01-06 from the population increases the mean age to 12.8 ka which falls within 1-sigma uncertainty of our reported age and therefore does not change our interpretations. Age of the Emerald Lake moraine calculated using the Titcomb



Lakes, WY production rate (TL; Gosse et al., 1995) yields a mean age and standard deviation of 11.6 ± 0.6 ka. This age difference of 0.9 ka between production rates has implications for the paleoclimatic interpretation. Here we discuss the paleoclimatic implications of both ages as it relates to glaciation within the Beartooth Mountains.

225 Samples ($n = 4$) from the Little Glacier Lake outer moraine yield exposure ages ranging from $1,061 \pm 39$ yrs to $2,253 \pm 62$ yrs (Table 1). Sample LGL-BT-07-17 ($1,061 \pm 39$ yrs) is identified as an outlier and excluded from the population. The mean age and uncertainty of the remaining distribution is $2,063 \pm 178$ yrs.

230 The inner Little Glacier Lake moraine yielded four exposure ages ranging from 724 ± 49 yrs to $1,354 \pm 47$ yrs (Table 1). A ~ 600 yr range exists between the oldest and youngest age of the population, however, no samples are rejected using the statistical tests described. These samples were likely affected by geologic processes. One possible explanation is some boulders contain accumulated nuclides from previous periods of exposure and are perhaps sourced from rock fall from the nearby cirque headwall and cliff faces. If this is the case, the youngest ages from the moraine are most likely to represent a period of glaciation. Based on geomorphological characteristics, including the bouldery nature and steep toe of the moraine, another possibility is that this moraine is the product of rock glaciation with lower rates of erosion less likely to remove previously accumulated nuclides from past periods of exposure. The sample population as a whole demonstrates a multi-modal distribution, which could be interpreted as numerous periods of glaciation. However, we offer a more conservative interpretation and consider the youngest age as a minimum limiting age of glaciation for this particular glacier in the Upper Valley.

235 240 Five samples from the moraine near Triangle Lake yield exposure ages ranging from 120 ± 13 yrs to $2,156 \pm 67$ yrs. Sample TrL-07-17 ($2,156 \pm 67$ yrs) is identified as an outlier using both previously mentioned statistical tests. The four remaining samples exhibit an approximate bimodal distribution, but overlap within 2-sigma uncertainty. Therefore, we interpret the mean age of 249 ± 126 yrs for all four samples.

245 Choice of production rate for our ages has little effect on the Little Glacier Lake and Triangle Lake moraines with each moraine age changing by fewer than 100 years (Table 2).

5 Discussion

5.1 Variable rates of western U.S. glacier retreat from the LGM to the Younger Dryas

250 During the last deglaciation the timing and rate of retreat of western U.S. glaciers varied spatially (Laabs et al., 2020). Broadly, glacial retreat from LGM margins in the western U.S. began between 22 ka and 18 ka (Shakun et al., 2015; Young et al., 2011). Glaciers from the northern GYGS fall within this window of deglacial onset, with two terminal moraines yielding ^{10}Be exposure ages of 19.8 ± 0.9 ka and 18.2 ± 1.3 ka (Fig. 5; Licciardi and Pierce, 2018). While no geochronologic control exists for the lateral moraines near Red Lodge, a lack of moraines outboard of them suggest they represent a terminal position of the glacier. They are also morphologically similar to other LGM-mapped moraines within the Beartooths (Black Butte; 25 km west of Red Lodge), and are proximal to the dated moraines at Clarks Fork (19.8 ± 0.9 ka) and Pine Creek (18.2 ± 1.3 ka) that are part of the same regional glacial system. Therefore, for our purposes, we assume the age, and therefore the onset of deglaciation, of the Red Lodge moraines to fall within the time window of 22 ka to 18 ka.



Table 1 - Sample data and ¹⁰ Be concentrations									
Sample name	Latitude (DD)	Longitude (DD)	Elevation (m)	Thickness (cm)	Shielding	Date	Conc. (atoms g ⁻¹)	Conc. unc. (atoms g ⁻¹)	
<i>Triangle Lake^a</i>									
TrL-02-17	45.00993	-109.55342	3064	2	0.937	2017	17996	992	
TrL-03-17	45.01003	-109.55327	3056	2	0.939	2017	5229	560	
TrL-05-17	45.01023	-109.55276	3049	5	0.939	2017	14573	850	
TrL-06-17	45.01021	-109.55286	3049	4	0.939	2017	7370	647	
TrL-07-17	45.01039	-109.55219	3058	2	0.939	2017	84217	2632	
<i>Little Glacier Lake - outer^a</i>									
LGL-BT-02-17	44.9983	-109.533	3042	2	0.981	2017	81645	2443	
LGL-BT-04-17	44.99907	-109.53428	3023	2	0.951	2017	53327	1863	
LGL-BT-05-17	44.9989	-109.5346	3045	2	0.96	2017	74396	2668	
LGL-BT-06-17	44.9981	-109.5369	3057	2	0.909	2017	85516	2366	
LGL-BT-07-17	44.9986	-109.5362	3060	2	0.938	2017	45089	1664	
<i>Little Glacier Lake - inner^b</i>									
LGL-BT-01-06	44.99698	-109.53462	3094	2	0.891	2006	33396	5584	
LGL-BT-02-06	44.99728	-109.53433	3075	2	0.891	2006	31674	2156	
LGL-BT-03-06	44.99772	-109.53322	3057	2	0.935	2006	47683	3620	
<i>Emerald Lake^b</i>									
EL-BT-01-06	44.99887	-109.52185	2999	2	0.969	2006	477331	8107	
EL-BT-02-06	44.99957	-109.52243	2993	2	0.989	2006	517609	8749	
EL-BT-03-06	44.99957	-109.5233	2990	2	0.989	2006	537278	9494	
EL-BT-06-06	44.99892	-109.52802	2989	2	0.977	2006	528085	14047	
EL-BT-07-06	44.99885	-109.52743	2991	2	0.977	2006	533612	21843	
<i>Blanks</i>									
Blank-004	-	-	-	-	-	-	54395	10291	
Blank-005	-	-	-	-	-	-	37559	8405	
Blank-024	-	-	-	-	-	-	30634	5901	
^a Samples that used Blank-024 in calculations									
^b Samples that used Blank-004 and Blank-005 in calculations									

260

265

270

275

280

Rapid retreat of the Clarks Fork glacier to the Crandall Creek moraine between 19.8 ± 0.9 ka and 18.2 ± 0.8 ka was followed by the construction of multiple recessional moraines as retreat slowed (Licciardi and Pierce, 2018). Initial, rapid retreat of the Clarks Fork glacier is hypothesized to have occurred as migration of the Yellowstone Ice Cap to the southwest created a precipitation shadow for the northeast portion of the GYGS thus affecting glacial mass balance negatively (Licciardi and Pierce, 2018, 2008). Synchronous changes in North American precipitation patterns were affecting glacial mass balance in the central north region of the U.S. (Lora and Ibarra, 2019). These changes in precipitation include migration of the dominant atmospheric jet stream (Lora et al., 2017) and changes in the seasonality of precipitation delivery to certain regions (Lora and Ibarra, 2019). Slower retreat of the Clarks Fork glacier during the Late Pinedale (16-13 ka) is attributed to a reduction of the precipitation shadow in the northeast GYGS as the Yellowstone Ice Cap continued its migration to the southwest (Licciardi and Pierce, 2018). After ~14 ka a more regionally coherent response of glacier retreat occurred in response to warming from increased atmospheric greenhouse gas concentrations (Marcott et al., 2019, 2014; Shakun et al., 2015).

Graf (1971) mapped five moraines within the Lower Valley between our prescribed LGM moraines and the Upper Valley which mark the location of the glacier as it retreated from its terminal position (Fig. 1). Based on geomorphological evidence such as distance regression, soil development, and shape index, the two furthest down valley moraines were associated with Bull Lake glaciation and the three more upvalley moraines as Pinedale terminal moraines. Furthermore, Graf (1971) assigned the Pinedale moraines correlative ages with other Western U.S. deposits ranging from 23.0 ka for the outermost to 11.5 ka for a moraine found near the steep transition from Lower to Upper Valley. However, based on the reasons described above, we argue all deposits within the Lower Valley are more likely

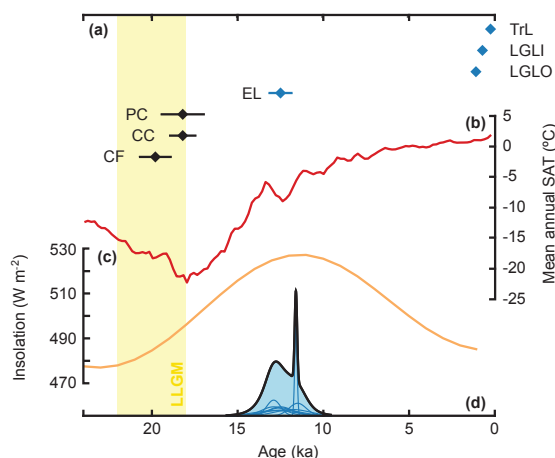


representative of post-LGM deglaciation similar to proximal glacial valleys within the GYGS (Laabs et al., 2020; Licciardi and Pierce, 2018, 2008). Additionally, the age of glacial retreat we obtained for the Emerald Lake moraine (12.5 ± 0.7 ka) inboard from the Graf (1971) 11.5 ka Lower Valley moraine suggests stabilization of the glacial prior to 12.5 ± 0.7 ka and is therefore in stratigraphic disagreement with this assigned age. As such, the Lower Valley deposits must be older than 12.5 ± 0.7 ka, and represent a period of glaciation between the end of the LGM (22 ka to 18 ka) and formation of the Emerald Lake moraine (Fig. 5).

The five Lower Valley moraines between Red Lodge and the Upper Valley suggest multiple periods of stagnation or glacial readvance during the last deglaciation. A lack of numerical age control limits our ability to assess the rate and timing of retreat within the Lower Valley. However, stratigraphic relationships of the moraines along with chronologic control higher in the valley permit a certain amount of bookending.

The Emerald Lake moraine marks the next geochronologically-constrained position of the glacier following the LGM. Using the time window of 22 ka to 18 ka for the onset of LGM deglaciation in Red Lodge and the age of the Emerald Lake moraine as limiting ages we determined a maximum and minimum mean retreat rate of the glacier of 4.9 m/yr (18.0 – 12.5 ka) and 2.8 m/yr (22.0 – 11.6 ka), respectively. These values are lower than those recorded for the nearby Clarks Fork glacier, which lost 75-90% of its LGM length between 19.8 ± 0.9 ka and 18.2 ± 0.8 ka at a mean retreat rate of 28.0 m/yr (Licciardi and Pierce, 2018).

We hypothesize that retreat of the Rock Creek glacier from its LGM limit began later in the window of LGM retreat (22 to 18 ka) similar to the Pine Creek moraine (18.2 ± 1.3 ka), experienced slower retreat similar to that of the Clarks Fork glacier after abandoning the Crandall Creek moraine (18.2 ± 0.8 ka), thus allowing for the formation of morainal features within the Lower Valley, and eventually left the Lower Valley in response to rising atmospheric greenhouse gases.



305 **Fig. 5 - LGM, Deglacial, and Holocene- Diamonds indicate moraine ages. (a) Blue diamonds are ages from this study. TrL = Triangle Lake, LGLI = Little Glacier Lake inner moraine, LGLO = Little Glacier Lake outer moraine. Black diamonds are ages from Licciardi & Pierce (2018). PC = Pine Creek moraine, CC = Crandall Creek, CF = Clarks Fork. (b) Red line is mean annual surface temperature for our study area taken from**



310 **Osman et al. (2021). (c) Orange line is mean annual insolation for 45° N. (d) Bottom probability distribution shaded in blue is for the compilation of western U.S. Younger Dryas moraines taken from Marcott et al. (2019), Licciardi and Pierce (2018), and the Emerald Lake moraine from this study. Yellow box highlights the timing of the local LGM from 22 ka to 18 ka.**

5.2 The Younger Dryas

315 Presence of the Emerald Lake moraine shows the location of the glacier in the latest Pleistocene, older than the previously proposed Neoglacial age (Graf, 1971), and marks a pinning point of glaciation during retreat from the LGM limits. Additionally, these data contribute to a growing data set of western U.S. moraine ages supporting a regional response of mountain glaciers to the YD (Marcott et al., 2019),

320 The Emerald Lake moraine marks the first location of the glacier margin in the Upper Valley ~27 km upvalley from the LGM position. Presence of the moraine indicates stillstand or readvance of the glacier during the latest Pleistocene, perhaps in response to Younger Dryas (YD) cooling (12.9 – 11.7 ka; Davis et al., 2009; Gosse et al., 1995). Geochronologic studies from glaciers in additional western U.S. mountain ranges identify similar glacier responses to YD cooling (Gosse et al., 1995; Licciardi and Pierce, 2008; Marcott et al., 2019) while other paleoclimate proxies identify a YD signal in the region (Mix et al., 1999; Praetorius et al., 2020, 2015; Vacco et al., 2005). However, 325 uncertainty of the exposure ages, and differences in production rate calculations, prevent conclusively attributing formation of the Emerald Lake moraine to the early- or later-portions of the YD stadial. Two potential scenarios arise: (1) deposition of the moraine early in the YD cooling with glacier retreat continuing throughout the stadial, and (2) deposition in response to YD cooling and retreat following abrupt warming at the end of the YD.

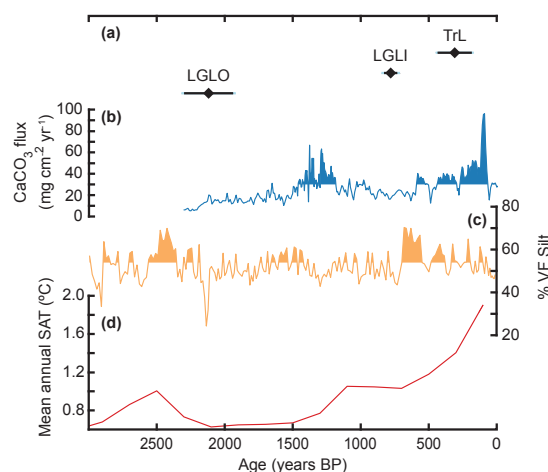
330 The age of the Emerald Lake moraine reported using the PPT production rate places retreat of the glacier from this location 12.5 ± 0.7 ka with glacial stagnation occurring prior to this time (Fig. 5). Morainal deposits near the Lake Solitude cirque lip in the nearby Teton Range (~175 km to the south) are dated to 12.9 ± 0.7 ka (Licciardi and Pierce, 2008; recalculated in Licciardi and Pierce, 2018). Together the ages of the Emerald Lake and Lake Solitude moraines imply a glacier response to the YD cooling with retreat during, or after, the stadial. A compilation of YD-age deposits from the western U.S. (Marcott et al., 2019), calculated using the PPT production rate and LSDn scaling 335 scheme, highlight 9 separate moraine exposure ages (including the Emerald Lake and Lake Solitude moraines) between 12.9 ± 0.7 ka (Licciardi and Pierce, 2008) and 11.5 ± 0.5 ka (Marcott et al., 2019). Mean age and standard deviation of these moraines are 12.3 ± 0.6 ka, while probability density indicates a higher peak earlier in the stadial (12.8 ka). All moraines in the compilation exist between 37–45° N and above 2765 m elevation. Taken together, these exposure ages suggest a regional glacial response to the YD stadial, with variability in timing of morainal 340 abandonment– potentially driven by differences in precipitation patterns (Lora and Ibarra, 2019), atmospheric lapse rate (Loomis et al., 2017; Zhang et al., 2019), or topographic control (Barr and Spagnolo, 2015).

345 Age of the Emerald Lake moraine calculated using the TL production rate (11.6 ± 0.6 ka) indicates retreat of the glacier later in the YD. Even with consideration of age uncertainty, the reported exposure age highlights moraine abandonment ~700 years after the onset of the YD stadial at a minimum (Fig. 5). As such, the glacier potentially stabilized in response to abruptly suppressed temperatures, maintained its position for > 700 years, and retreated as temperatures recovered at the end of the stadial. However, the deflated nature of the Emerald Lake moraine lies in contrast to the much younger Triangle and Frosty Lake moraines, as well as to the older LGM moraines found at



350

Clarks Fork and Black Butte. Similar low-profile morainal deposits associated with mountain glaciation are attributed to high-frequency glacier length variability during deglaciation (Barth et al., 2018). Therefore, the subdued profile of the Emerald Lake moraine suggests any period of stagnation was short-lived and/or characterized by low depositional rates. Any forcing of this response had minor impact in the overall trend of glacier retreat.



355

Fig. 6 - Neoglacial – (a) Ages for the late-Holocene moraines from this study adjusted to reflect years before present. Black lines indicate 1-sigma analytic uncertainty. Light blue lines in the ages include the production rate uncertainty added in quadrature. (b) Blue line shows the CaCO₃ flux from Harrison Lake in Glacier National Park (Munroe et al., 2012). Shaded areas indicate greater than mean values for the time series and interpreted as increased glacial activity in the original study. (c) Orange line shows the percent very fine silt fraction from Cracker Lake in Glacier National Park (Munroe et al., 2012). Shaded areas indicate greater than mean values and increased glacial activity. (d) Red line is the mean annual surface temperature for our study region taken from Osman et al. (2021).

360

5.3 Constraints on Neoglaciation and the Little Ice Age

365

Ages from the Little Glacier Lake and Triangle Lake moraines indicate Upper Valley glacier activity within the late Holocene. Glaciation in the western U.S. is suggested to have reached a minimum in the early Holocene due to high Northern Hemisphere summer insolation (Fig., 6; Porter and Denton, 1967). Multiple archives across the northern hemisphere highlight a readvance of glaciers in the later Holocene (Munroe et al., 2012; Porter and Denton, 1967; Reyes et al., 2006; Solomina et al., 2015) due to declining summer temperatures (Marcott et al., 2013; McKay et al., 2018). Late-Holocene, Neoglacial deposits are found in numerous mountain ranges across the western U.S. and Canada, Greenland, Europe, and Asia (Briner and Porter, 2018; Graf, 1971; Marcott et al., 2019; Munroe et al., 2012; Reyes et al., 2006; Solomina et al., 2015).

370

375

Age of the Little Glacier Lake outer moraine indicates conditions within the Upper Valley had become favorable for glacier activity by $2,063 \pm 178$ years ago with glaciation likely occurring prior to this time. This age also implies that subsequent glaciation (e.g., LIA) did not exceed this boundary which therefore represents the maximum late-Holocene glacial extent. Based on geomorphic evidence and variability among exposure ages, we suggest that the Little Glacier Lake inner moraine represents rock glaciation which form through transitional glacial and periglacial



380

processes (Petersen et al., 2020). Conservatively, we assume the youngest ages within the distribution act as minimum-limiting constraints on the timing of glaciation after the abandonment of the outer moraine. Therefore, continued and variable glacial-periglacial conditions for the Little Glacier Lake rock glacier is demonstrated by the youngest exposure ages from the inner deposit (724 ± 49 yrs; Fig. 6).

385

In nearby Glacier National Park, MT (~500 km north of the Beartooth Mountains) proglacial lake sediments are interpreted to indicate glacier fluctuations throughout the Holocene including phases of glacier advance 2,300 and 1,500 cal year BP and again after 700 cal year BP (Fig. 5; Munroe et al., 2012). Paleo-proxy reconstructions of temperature and precipitation for the region indicate lower than average temperatures and increased winter precipitation ~1,600-1,200 years ago with continued decreased temperatures ~700 years ago (Trouet et al., 2013; Viau et al., 2012). Such conditions present favorable climates for glaciation and correlate with the timing of Little Glacier Lake activity.

390

Continuation of climate/glacier variability recorded in ages of the Little Glacier Lake deposits and regional paleoproxies culminated with the glaciation recorded in the Triangle Lake moraine. Morainal abandonment of the Triangle Lake glacier 249 ± 126 yrs ago marks the end of substantial moraine construction within the Upper Valley. Similarities between the Triangle Lake and the upvalley Frosty Lake moraine morphologies imply similar age and behavior of the two glaciers. Both moraines are large (>50 m relief) likely from either long duration of moraine construction at the boundary or high depositional rates. We suggest late-Holocene reactivation of the Triangle Lake glacier was synchronous with the onset of glaciation recorded in the Little Glacier Lake deposits as both responded to the same forcing. Unlike at Little Glacier Lake, the Triangle Lake glacier maintained its position and positive mass balance longer, thus constructing a more substantial moraine and staving off rock glaciation, which can occur as a periglacial feature (Giardino and Vitek, 1988; Knight et al., 2019).

395

400

A recent study of glaciers in New Zealand highlight the inverse hemispheric relationship as those glaciers reached maximum lengths early in the Holocene and retreated ever since (Dowling et al., 2021). It is likely that glaciers and periglacial features in the higher elevations of the Beartooth Mountains reactivated in response to late-Holocene low NH insolation levels, and provide evidence of cooler, and more favorable, climates in the last half of the Holocene. Though proximal, differences in Little Glacier Lake and Triangle Lake glacier response to climate forcing could be driven by the influence of higher, and more shaded, headwalls surrounding the Triangle Lake glacier. Similar influence of topography have been shown to influence alpine glacier advances (Barr and Spagnolo, 2015). Taken together, the Little Glacier Lake and Triangle Lake exposure ages suggest reactivation of glaciers within the Upper Valley from their early Holocene minima during the Neoglaciation prior to $2,063 \pm 178$ yrs with deglaciation occurring as late as 249 ± 126 yrs. Exposure ages from the Little Glacier Lake inner deposit support regional studies suggestive of glacier fluctuations and climate variability throughout the Neoglaciation.

405

410 6 Conclusion

New ^{10}Be surface exposure ages from the Rock Creek drainage in the eastern Beartooth mountain range yield new insight into the timing of western U.S. glaciation. After likely retreating from the LGM limit between 22 ka and 18 ka, the glacier stabilized in the Upper Valley early in the Younger Dryas stadial as evidenced by the Emerald Lake



415 moraine (12.5 ± 0.7 ka). This age redefines the age of the deposit, which was initially suggested to be Neoglacial in
age by Graf (1971), and fits a trend of previously assigned Neoglacial deposits being geochronologically constrained
to latest Pleistocene and earliest Holocene glaciation (Marcott et al., 2019). Evidence of Neoglaciation is found within
the Upper Valley in the presence Little Glacier Lake outer moraine that yields an age of $2,063 \pm 178$ yrs, and continued
glacial-periglacial rock glacier fluctuations occurring throughout the late Holocene (724 ± 49 yrs). These deposits
support evidence that climatic conditions within the western U.S. were favorable for glaciation at high elevations in
420 the late Holocene (Marcott et al., 2019; Solomina et al., 2016). Glaciation continued within the Upper Valley until
retreat of the Triangle Lake glacier 249 ± 126 yrs, with only ephemeral glaciers and ice patches remaining today.

Data availability

Data from this study including those used in the figures are available in the Supplement.

425

Supplement link

The supplement related to this article is available online.

Author contributions

430 AMB: Conceptualization, Investigation, Writing – Original Draft, Visualization, Funding acquisition. EGC:
Investigation, Writing – Review and Editing. CV: Investigation, Writing – Review and Editing. SAM:
Conceptualization, Investigation, Writing – Review and Editing, Funding acquisition. JDS: Conceptualization,
Investigation, Writing – Review and Editing. MWC: Investigation, Writing – Review and Editing.

435 Competing interests

The authors declare that they have no conflict of interest.

References

- 440 Balco, G., Stone, J.O., Lifton, N.A., Dunai, T.J., 2008. A complete and easily accessible means of calculating
surface exposure ages or erosion rates from ^{10}Be and ^{26}Al measurements. *Quaternary Geochronology* 3,
174–195. <https://doi.org/10.1016/j.quageo.2007.12.001>
- Ballantyne, C.K., Stone, J.O., 2012. Did large ice caps persist on low ground in north-west Scotland during the
Lateglacial Interstade? *Journal of Quaternary Science* 27, 297–306. <https://doi.org/10.1002/jqs.1544>
- 445 Ballard, G.A., 1976. Evidence to suggest catastrophic flooding of Clarks Fork of the Yellowstone River,
northeastern Wyoming (M.S.). University of Utah.
- Barr, I.D., Spagnolo, M., 2015. Glacial cirques as palaeoenvironmental indicators: Their potential and limitations.
Earth-Science Reviews 151, 48–78. <https://doi.org/10.1016/j.earscirev.2015.10.004>
- Barth, A.M., Clark, P.U., Clark, J., Roe, G.H., Marcott, S.A., McCabe, A.M., Caffee, M.W., He, F., Cuzzone, J.K.,
Dunlop, P., 2018. Persistent millennial-scale glacier fluctuations in Ireland between 24 ka and 10 ka. *Geology*
46, 151–154. <https://doi.org/10.1130/G39796.1>
- 450 Barth, A.M., Marcott, S.A., Licciardi, J.M., Shakun, J.D., 2019. Deglacial Thinning of the Laurentide Ice Sheet in
the Adirondack Mountains, New York, USA, Revealed by ^{36}Cl Exposure Dating. *Paleoceanography and
Paleoclimatology* 34, 946–953. <https://doi.org/10.1029/2018PA003477>
- 455 Bevan, A., 1923. Summary of the Geology of the Beartooth Mountains, Montana. *The Journal of Geology* 31, 441–
465. <https://doi.org/10.1086/623038>
- Bolch, T., 2007. Climate change and glacier retreat in northern Tien Shan (Kazakhstan/Kyrgyzstan) using remote
sensing data. *Global and Planetary Change* 56, 1–12. <https://doi.org/10.1016/j.gloplacha.2006.07.009>



- 460 Braumann, S.M., Schaefer, J.M., Neuhuber, S.M., Reitner, J.M., Lüthgens, C., Fiebig, M., 2020. Holocene glacier change in the Silvretta Massif (Austrian Alps) constrained by a new ^{10}Be chronology, historical records and modern observations. *Quaternary Science Reviews* 245, 106493. <https://doi.org/10.1016/j.quascirev.2020.106493>
- Briner, J.P., Porter, S.C., 2018. Neoglaciation in the American Cordilleras, in: *Encyclopedia of Quaternary Science*. Elsevier, pp. 1133–1142. <https://doi.org/10.1016/B0-444-52747-8/00137-X>
- 465 Catania, G.A., Stearns, L.A., Sutherland, D.A., Fried, M.J., Bartholomaeus, T.C., Morlighem, M., Shroyer, E., Nash, J., 2018. Geometric Controls on Tidewater Glacier Retreat in Central Western Greenland. *J. Geophys. Res. Earth Surf.* 123, 2024–2038. <https://doi.org/10.1029/2017JF004499>
- Clark, P.U., Dyke, A.S., Shakun, J.D., Carlson, A.E., Clark, J., Wohlfarth, B., Mitrovica, J.X., Hostetler, S.W., McCabe, A.M., 2009. The Last Glacial Maximum. *Science* 325, 710–4. <https://doi.org/10.1126/science.1172873>
- 470 Corbett, L.B., Bierman, P.R., Rood, D.H., 2016. An approach for optimizing in situ cosmogenic ^{10}Be sample preparation. *Quaternary Geochronology* 33, 24–34. <https://doi.org/10.1016/j.quageo.2016.02.001>
- Davis, P., 1988. Holocene glacier fluctuations in the American Cordillera. *Quaternary Science Reviews* 7, 129–157. [https://doi.org/10.1016/0277-3791\(88\)90003-0](https://doi.org/10.1016/0277-3791(88)90003-0)
- 475 Davis, P.T., Menounos, B., Osborn, G., 2009. Holocene and latest Pleistocene alpine glacier fluctuations: a global perspective. *Quaternary Science Reviews* 28, 2021–2033. <https://doi.org/10.1016/j.quascirev.2009.05.020>
- Dowling, L., Eaves, S., Norton, K., Mackintosh, A., Anderson, B., Hidy, A., Lorrey, A., Vargo, L., Ryan, M., Tims, S., 2021. Local summer insolation and greenhouse gas forcing drove warming and glacier retreat in New Zealand during the Holocene. *Quaternary Science Reviews* 266, 107068. <https://doi.org/10.1016/j.quascirev.2021.107068>
- 480 Dunai, T.J., 2010. *Cosmogenic Nuclides: Principles, Concepts and Applications in the Earth Surface Sciences*. Cambridge University Press, United Kingdom.
- Giardino, J.R., Vitek, J.D., 1988. The significance of rock glaciers in the glacial-periglacial landscape continuum. *J. Quaternary Sci.* 3, 97–103. <https://doi.org/10.1002/jqs.3390030111>
- 485 Gosse, J.C., Evenson, E.B., Klein, J., Lawn, B., Middleton, R., 1995. Precise cosmogenic ^{10}Be measurements in western North America: Support for a global Younger Dryas cooling event. *Geology* 23, 877–880.
- Gosse, J.C., Phillips, F.M., 2001. Terrestrial in situ cosmogenic nuclides: theory and application. *Quaternary Science Reviews* 20, 1475–1560.
- Graf, W.L., 1971. Quantitative Analysis of Pinedale Landforms, Beartooth Mountains, Montana and Wyoming. *Arctic and Alpine Research* 3, 253. <https://doi.org/10.2307/1550197>
- 490 Hugonnet, R., McNabb, R., Berthier, E., Menounos, B., Nuth, C., Girod, L., Farinotti, D., Huss, M., Dussailant, I., Brun, F., Käab, A., 2021. Accelerated global glacier mass loss in the early twenty-first century. *Nature* 592, 726–731. <https://doi.org/10.1038/s41586-021-03436-z>
- Knight, J., Harrison, S., Jones, D.B., 2019. Rock glaciers and the geomorphological evolution of deglaciating mountains. *Geomorphology* 324, 14–24. <https://doi.org/10.1016/j.geomorph.2018.09.020>
- 495 Kohl, C.P., Nishiizumi, K., 1992. Chemical isolation of quartz for measurement of in-situ-produced cosmogenic nuclides. *Geochimica et Cosmochimica Acta* 56, 3583–3587.
- Laabs, B.J.C., Licciardi, J.M., Leonard, E.M., Munroe, J.S., Marchetti, D.W., 2020. Updated cosmogenic chronologies of Pleistocene mountain glaciation in the western United States and associated paleoclimate inferences. *Quaternary Science Reviews* 242, 106427. <https://doi.org/10.1016/j.quascirev.2020.106427>
- 500 Licciardi, J., 2000. *Alpine Glacier and Pluvial Lake Records of Late Pleistocene Climate Variability in the Western United States (Dissertation)*. Oregon State University.
- Licciardi, J.M., Pierce, K.L., 2018. History and dynamics of the Greater Yellowstone Glacial System during the last two glaciations. *Quaternary Science Reviews* 200, 1–33. <https://doi.org/10.1016/j.quascirev.2018.08.027>
- Licciardi, J.M., Pierce, K.L., 2008. Cosmogenic exposure-age chronologies of Pinedale and Bull Lake glaciations in greater Yellowstone and the Teton Range, USA. *Quaternary Science Reviews* 27, 814–831. <https://doi.org/10.1016/j.quascirev.2007.12.005>
- 505 Lifton, N., Caffee, M., Finkel, R., Marrero, S., Nishiizumi, K., Phillips, F.M., Goehring, B., Gosse, J., Stone, J., Schaefer, J., Theriault, B., Jull, A.J.T., Fifield, K., 2015. In situ cosmogenic nuclide production rate calibration for the CRONUS-Earth project from Lake Bonneville, Utah, shoreline features. *Quaternary Geochronology* 26, 56–69. <https://doi.org/10.1016/j.quageo.2014.11.002>
- 510 Lifton, N., Sato, T., Dunai, T.J., 2014. Scaling in situ cosmogenic nuclide production rates using analytical approximations to atmospheric cosmic-ray fluxes. *Earth and Planetary Science Letters* 386, 149–160. <https://doi.org/10.1016/j.epsl.2013.10.052>



- 515 Loomis, S.E., Russell, J.M., Verschuren, D., Morrill, C., De Cort, G., Sinninghe Damsté, J.S., Olago, D.,
Eggermont, H., Street-Perrott, F.A., Kelly, M.A., 2017. The tropical lapse rate steepened during the Last
Glacial Maximum. *Sci. Adv.* 3, e1600815. <https://doi.org/10.1126/sciadv.1600815>
- Lora, J.M., Ibarra, D.E., 2019. The North American hydrologic cycle through the last deglaciation. *Quaternary
Science Reviews* 226, 105991. <https://doi.org/10.1016/j.quascirev.2019.105991>
- 520 Lora, J.M., Mitchell, J.L., Risi, C., Tripathi, A.E., 2017. North Pacific atmospheric rivers and their influence on
western North America at the Last Glacial Maximum. *Geophys. Res. Lett.* 44, 1051–1059.
<https://doi.org/10.1002/2016GL071541>
- Marcott, S.A., 2011. Late Pleistocene and Holocene Glacier and Climate Change. Oregon State University.
- Marcott, S.A., Bauska, T.K., Buizert, C., Steig, E.J., Rosen, J.L., Cuffey, K.M., Fudge, T.J., Severinghaus, J.P.,
525 Ahn, J., Kalk, M.L., McConnell, J.R., Sowers, T., Taylor, K.C., White, J.W., Brook, E.J., 2014. Centennial-
scale changes in the global carbon cycle during the last deglaciation. *Nature* 514, 616–9.
<https://doi.org/10.1038/nature13799>
- Marcott, S.A., Clark, P.U., Shakun, J.D., Brook, E.J., Davis, P.T., Caffee, M.W., 2019. 10Be age constraints on
latest Pleistocene and Holocene cirque glaciation across the western United States. *npj Clim Atmos Sci* 2, 5.
<https://doi.org/10.1038/s41612-019-0062-z>
- 530 Marcott, S.A., Shakun, J.D., Clark, P.U., Mix, A.C., 2013. A reconstruction of regional and global temperature for
the past 11,300 years. *Science* 339, 1198–201. <https://doi.org/10.1126/science.1228026>
- McKay, N.P., Kaufman, D.S., Routson, C.C., Erb, M.P., Zander, P.D., 2018. The Onset and Rate of Holocene
Neoglacial Cooling in the Arctic. *Geophys. Res. Lett.* 45, 12,487–12,496.
<https://doi.org/10.1029/2018GL079773>
- 535 Mix, A.C., Lund, D.C., Pisias, N.G., Bodén, P., Bormmalm, L., Lyle, M., Pike, J., 1999. Rapid climate oscillations in
the Northeast Pacific during the last deglaciation reflect Northern and Southern Hemisphere sources, in:
Rapid Climate Oscillations in the Northeast Pacific during the Last Deglaciation Reflect Northern and
Southern Hemisphere Sources, AGU Monograph. American Geophysical Union, Washington, D. C., pp.
127–148.
- 540 Montgomery, C.W., Lytwyn, J.N., 1984. Rb-Sr Systematics and Ages of Principal Precambrian Lithologies in the
South Snowy Block, Beartooth Mountains. *The Journal of Geology* 92, 103–112.
<https://doi.org/10.1086/628837>
- Munroe, J.S., Crocker, T.A., Giesche, A.M., Rahlson, L.E., Duran, L.T., Bigl, M.F., Laabs, B.J.C., 2012. A
lacustrine-based Neoglacial record for Glacier National Park, Montana, USA. *Quaternary Science Reviews*
545 53, 39–54. <https://doi.org/10.1016/j.quascirev.2012.08.005>
- Nishiizumi, K., Imamura, M., Caffee, M.W., Southon, J.R., Finkel, R.C., McAninch, J., 2007. Absolute calibration of
10Be AMS standards. *Nuclear Instruments and Methods in Physics Research Section B: Beam Interactions
with Materials and Atoms* 258, 403–413. <https://doi.org/10.1016/j.nimb.2007.01.297>
- 550 Petersen, E.I., Levy, J.S., Holt, J.W., Stuurman, C.M., 2020. New insights into ice accumulation at Galena Creek
Rock Glacier from radar imaging of its internal structure. *J. Glaciol.* 66, 1–10.
<https://doi.org/10.1017/jog.2019.67>
- Porter, S.C., Denton, G.H., 1967. Chronology of neoglaciation in the North American Cordillera. *American Journal
of Science* 265, 177–210.
- 555 Praetorius, S.K., Condron, A., Mix, A.C., Walczak, M.H., McKay, J.L., Du, J., 2020. The role of Northeast Pacific
meltwater events in deglacial climate change. *Sci. Adv.* 6, eaay2915. <https://doi.org/10.1126/sciadv.aay2915>
- Praetorius, S.K., Mix, A.C., Walczak, M.H., Wolhowe, M.D., Addison, J.A., Prah, F.G., 2015. North Pacific
deglacial hypoxic events linked to abrupt ocean warming. *Nature* 527, 362–6.
<https://doi.org/10.1038/nature15753>
- 560 Reyes, A.V., Wiles, G.C., Smith, D.J., Barclay, D.J., Allen, S., Jackson, S., Larocque, S., Laxton, S., Lewis, D.,
Calkin, P.E., Clague, J.J., 2006. Expansion of alpine glaciers in Pacific North America in the first millennium
A.D. *Geol* 34, 57. <https://doi.org/10.1130/G21902.1>
- Shakun, J.D., Clark, P.U., He, F., Lifton, N.A., Liu, Z., Otto-Bliesner, B.L., 2015. Regional and global forcing of
glacier retreat during the last deglaciation. *Nat Commun* 6, 8059. <https://doi.org/10.1038/ncomms9059>
- 565 Solomina, O.N., Bradley, R.S., Hodgson, D.A., Ivy-Ochs, S., Jomelli, V., Mackintosh, A.N., Nesje, A., Owen, L.A.,
Wanner, H., Wiles, G.C., Young, N.E., 2015. Holocene glacier fluctuations. *Quaternary Science Reviews*
111, 9–34. <https://doi.org/10.1016/j.quascirev.2014.11.018>
- Solomina, O.N., Bradley, R.S., Jomelli, V., Geirsdottir, A., Kaufman, D.S., Koch, J., McKay, N.P., Masiokas, M.,
Miller, G., Nesje, A., Nicolussi, K., Owen, L.A., Putnam, A.E., Wanner, H., Wiles, G., Yang, B., 2016.



- 570 Glacier fluctuations during the past 2000 years. *Quaternary Science Reviews* 149, 61–90.
<https://doi.org/10.1016/j.quascirev.2016.04.008>
- Trouet, V., Diaz, H.F., Wahl, E.R., Viau, A.E., Graham, R., Graham, N., Cook, E.R., 2013. A 1500-year reconstruction of annual mean temperature for temperate North America on decadal-to-multidecadal time scales. *Environmental Research Letters* 8, 024008. <https://doi.org/10.1088/1748-9326/8/2/024008>
- 575 Vacco, D.A., Clark, P.U., Mix, A.C., Cheng, H., Edwards, R.L., 2005. A speleothem record of Younger Dryas cooling, Klamath Mountains, Oregon, USA. *Quaternary Research* 64, 249–256.
- Van Gosen, B.S., Elliot, J.E., LaRock, E.J., du Bray, E.A., Carlson, R.R., Zientek, M.L., 2000. Generalized geologic map of the Absaroka-Beartooth study area, south-central Montana. <https://doi.org/10.3133/mf2338>
- Viau, A.E., Ladd, M., Gajewski, K., 2012. The climate of North America during the past 2000 years reconstructed from pollen data. *Global and Planetary Change* 84–85, 75–83.
<https://doi.org/10.1016/j.gloplacha.2011.09.010>
- 580 Young, N.E., Briner, J.P., Leonard, E.M., Licciardi, J.M., Lee, K., 2011. Assessing climatic and nonclimatic forcing of Pinedale glaciation and deglaciation in the western United States. *Geology* 39, 171–174.
<https://doi.org/10.1130/g31527.1>
- 585 Zhang, E., Chang, J., Shulmeister, J., Langdon, P., Sun, W., Cao, Y., Yang, X., Shen, J., 2019. Summer temperature fluctuations in Southwestern China during the end of the LGM and the last deglaciation. *Earth and Planetary Science Letters* 509, 78–87. <https://doi.org/10.1016/j.epsl.2018.12.024>